Report

Current Biology

Historical Genomes Reveal the Genomic Consequences of Recent Population Decline in Eastern Gorillas

Highlights

- Gorilla genomes from museum samples enabled measurement of temporal genomic erosion
- Genetic diversity declined and inbreeding increased in Grauer's gorillas
- The frequency of deleterious mutations increased significantly in Grauer's gorillas
- No temporal changes in genomic parameters were observed in the mountain gorilla

Authors

Tom van der Valk, David Díez-del-Molino, Tomas Marques-Bonet, Katerina Guschanski, Love Dalén

Correspondence

katerina.guschanski@ebc.uu.se (K.G.), love.dalen@nrm.se (L.D.)

In Brief

Van der Valk et al. investigate the genomic consequences of recent population decline using 100-year-old museum specimens. They find a reduction in genetic diversity, increase in inbreeding, and increase in deleterious mutations in the critically endangered Grauer's gorillas.

van der Valk et al., 2019, Current Biology *29*, 165–170
January 7, 2019
https://doi.org/10.1016/j.cub.2018.11.055

CellPress

Current Biology
Report

Historical Genomes Reveal the Genomic Consequences of Recent Population Decline in Eastern Gorillas

Tom van der Valk,[1] David Díez-del-Molino,[2] Tomas Marques-Bonet,[3,4,5,6] Katerina Guschanski,[1,7,8,9,*] and Love Dalén[2,7,8,*]
[1]Department of Ecology and Genetics (Animal ecology), Uppsala University, 752 36 Uppsala, Sweden
[2]Department of Bioinformatics and Genetics, Swedish Museum of Natural History, Box 50007, 10405 Stockholm, Sweden
[3]Institute of Evolutionary Biology (UPF-CSIC), PRBB, Dr. Aiguader 88, 08003 Barcelona, Spain
[4]Catalan Institution of Research and Advanced Studies (ICREA), Passeig de Lluís Companys, 23, 08010, Barcelona, Spain
[5]CNAG-CRG, Centre for Genomic Regulation (CRG), Barcelona Institute of Science and Technology (BIST), Baldiri i Reixac 4, 08028 Barcelona, Spain
[6]Institut Català de Paleontologia Miquel Crusafont, Universitat Autònoma de Barcelona, Edifici ICTA-ICP, c/ Columnes s/n, 08193 Cerdanyola del Vallès, Barcelona, Spain
[7]Senior author
[8]These authors contributed equally
[9]Lead Contact
*Correspondence: katerina.guschanski@ebc.uu.se (K.G.), love.dalen@nrm.se (L.D.)
https://doi.org/10.1016/j.cub.2018.11.055

SUMMARY

Many endangered species have experienced severe population declines within the last centuries [1, 2]. However, despite concerns about negative fitness effects resulting from increased genetic drift and inbreeding, there is a lack of empirical data on genomic changes in conjunction with such declines [3–7]. Here, we use whole genomes recovered from century-old historical museum specimens to quantify the genomic consequences of small population size in the critically endangered Grauer's and endangered mountain gorillas. We find a reduction of genetic diversity and increase in inbreeding and genetic load in the Grauer's gorilla, which experienced severe population declines in recent decades. In contrast, the small but relatively stable mountain gorilla population has experienced little genomic change during the last century. These results suggest that species histories as well as the rate of demographic change may influence how population declines affect genome diversity.

RESULTS AND DISCUSSION

In the last centuries, continuously increasing anthropogenic pressures have dramatically accelerated wild animal population losses, especially affecting large-bodied mammals [1, 2]. These population declines can have severe consequences for long-term species survival due to environmental and demographic stochastic events [3], the negative effects of reduced genetic diversity on fertility [4], resistance to infectious diseases [8], and adaptability to changing environments [5]. Moreover, natural selection is thought to be less efficient in small populations, which may increase the probability that deleterious alleles drift to fixation, further lowering the fitness of the population [6]. Maintaining genetic diversity is thus of considerable importance for species conservation [7]. However, the genomic consequences of rapid population decline, as faced by many species today, remain largely unexplored due to limited empirical data [9].

In this study, we directly quantify genomic changes within the last century in the two eastern gorillas: the critically endangered Grauer's (*Gorilla beringei graueri*) and the endangered mountain gorillas (*Gorilla beringei beringei*) [10] by sequencing whole genomes from historical specimens collected up to ca. 100 years ago and comparing them to present-day (modern) genomes [11, 12] (Figure 1A). After low-depth sequencing of 59 historical gorilla specimens (see Data S1), we selected samples from unrelated adult individuals displaying high endogenous DNA content and DNA quantity for uracil-DNA glycosylase (UDG) treatment and subsequent deep genome sequencing. Following whole-genome sequencing, we collapsed the obtained forward and reverse high-quality sequencing reads generated on the Illumina HiSeq X platform and aligned them to the gorilla reference genome [13]. For seven Grauer's and four mountain gorilla samples collected between 1910 and 1962 (median: 1923), we obtained adequate coverage (3.1–10.8 X) to infer genomic changes through time (see Data S1). We also included published modern genomes from eight Grauer's, seven mountain, and 17 western lowland gorillas (*Gorilla gorilla gorilla*) (see Data S1) [11], the last to be used as a comparative dataset.

To study changes in genetic diversity over time, we called genotype likelihoods and variants across all historical and modern samples. We filtered low-quality sites, recalibrated quality scores accounting for post-mortem DNA damage, and removed cytosine-phosphate-guanine (CpG) sites to limit possible biases from remaining DNA damage (Figures S1A and S1B) [14].

Using principal-component and admixture analyses based on genotype likelihoods, we found indications for the presence of population structure in historical Grauer's gorillas, corroborating

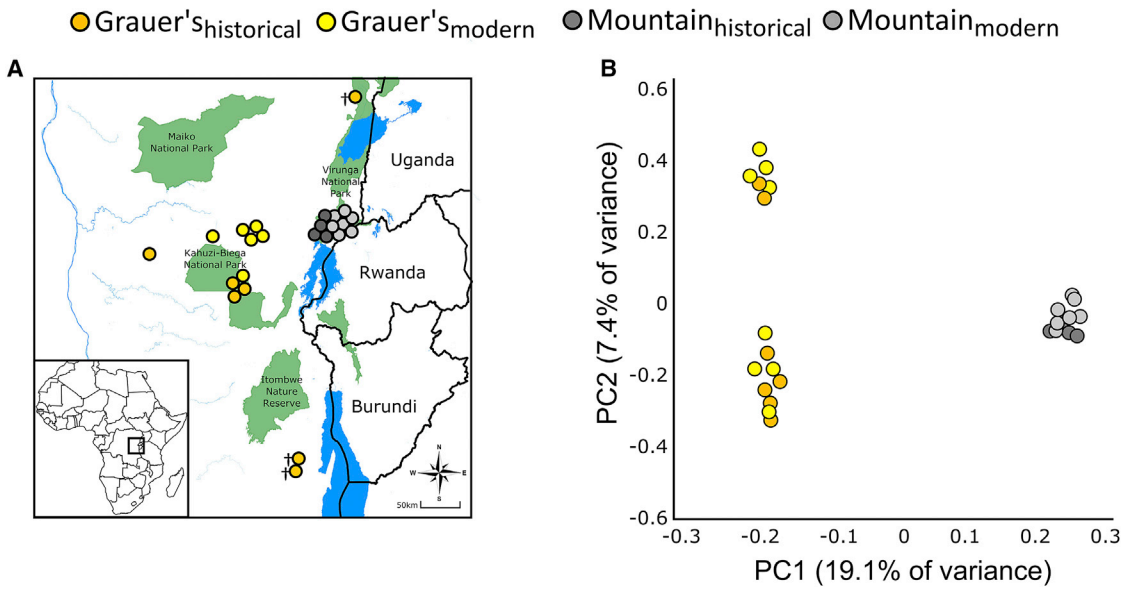

Figure 1. Geography and Genetic Structure

(A) Sampling location of historical and previously published modern samples. Two modern Grauer's gorilla individuals are not shown on the map due to uncertainty about their exact geographic origin. † depicts samples from extinct Grauer's gorilla populations.

(B) Principal-component analysis of eastern gorilla genomes.

See also Figure S2.

previous results based on modern data (Figures 1B and S2A–S2E) [12, 15]. Geography could not explain the apparent structure, as individuals from the extremes of the species distribution range were found to belong to the same genomic subcluster (Figures S2A and S2B). Next, we estimated the number of differences between chromosome pairs to assess intra-individual genetic diversity (heterozygosity) after downsampling modern samples to a similar coverage as the historical genomes to control for coverage biases (Figure S1C). We found a decline in autosomal heterozygosity in Grauer's gorillas, with modern individuals containing on average ~20% fewer heterozygous sites than historical individuals (Figures 2A and S1D). We also observed lower genetic diversity in modern mountain gorillas; however, the difference compared to the historical individuals was small (3%) and not statistically significant (Figures 2A and S1D). We obtained similar results independent of the method used to call genomic variants (Figure S1D), and we can exclude population substructure, difference in sample sizes, and retained post-mortem DNA damage as possible explanations (Figures S1C and S2F–S2H). Estimating diversity at population level as the total number of variable sites per population also supported the observed reduction in genetic diversity in the modern Grauer's gorillas compared to the historical samples (Figure S1E).

Next, we inferred the effects of the recent population decline on inbreeding levels by identifying tracts of within-individual chromosomal sequence sharing (runs of homozygosity [ROH]) using a Hidden Markov Model. Whereas an average of 35.1% and 33.9% of the historical Grauer's and mountain gorilla genomes, respectively, consisted of ROH above 100 kb, this proportion increased to 39.2% in modern Grauer's and to 36.3% in modern mountain gorillas (Figures 2B and S3). This change is driven by the proportion of the genome contained in very long ROH (2.5–10 Mb, Figures 2B–2C and S3), which increased by 24% in modern Grauer's gorilla genomes (Figures 2B and 2C). Such long tracts are likely to arise from mating between closely related individuals less than ten generations ago [16]. In regions of the genome outside of ROH, heterozygosity levels were similar between historical and modern Grauer's gorillas (Figure 2A), indicating that recent inbreeding is the main cause of the observed reduction in genome-wide genetic diversity. The proportion of the genome contained in long ROH increased by 6.9% in modern mountain gorillas; however, the difference with the historical samples was not statistically significant (Figures 2B and S3).

To test whether population decline and small population size led to an accumulation of deleterious mutations in eastern gorillas, we used three independent and complementary approaches to characterize genetic load on genome-wide, gene, and protein level. First, we estimated genetic load for each individual by measuring the proportion of homozygous-derived mutations in regions of the genome that are conserved across a whole-genome alignment of 20 vertebrates and thus can be assumed to be mostly deleterious [17]. Although the differences in genetic load between modern and historical eastern gorilla individuals were not significant, a larger proportion of modern genomes of both Grauer's and mountain gorillas fell into the upper range of the distribution (Figure 3A). Second, we assessed the effects of DNA sequence variants on protein-coding genes and found a significant increase in frequency of both missense and loss-of-function (LoF) variants in modern Grauer's gorillas compared to the historical individuals, consistent with higher genetic load in the modern population (Figure 3B). In contrast, our results suggest that the frequency of missense and LoF variants has remained stable in the mountain gorillas during the last

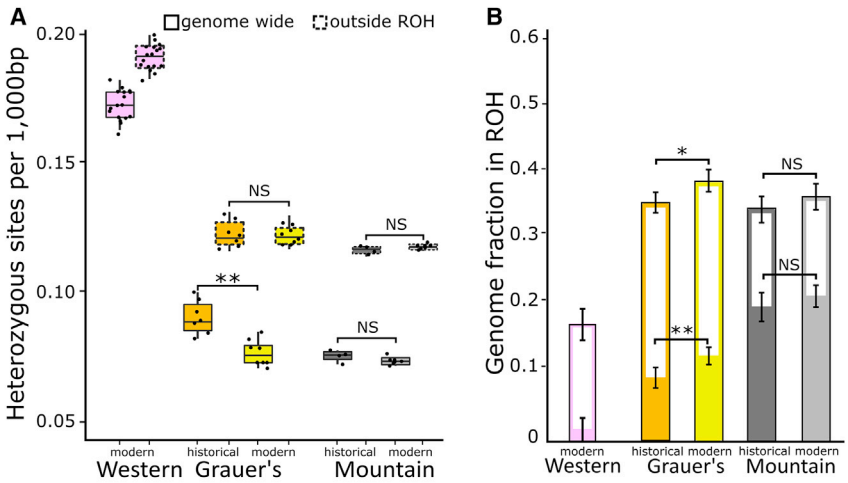

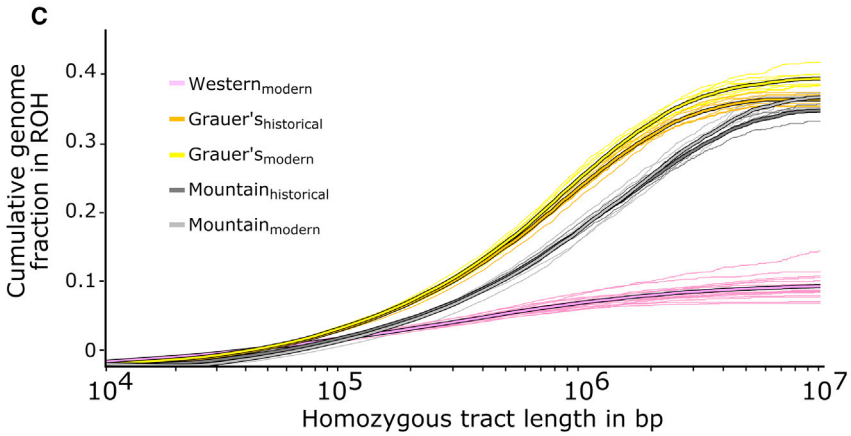

Figure 2. Temporal Genetic Diversity and Inbreeding

(A) Genome-wide heterozygosity of gorilla individuals (solid outlines) and heterozygosity excluding runs of homozygosity (ROH, dotted outlines). Each black dot represents one individual. **p < 0.01; NS, not significant.

(B) Fraction of the genomes in ROH above 100 kb (open bars), and long ROH between 2.5 and 10 Mb (solid bars). Error bars, ±1 SD. *p < 0.05, **p < 0.01; NS, not significant.

(C) Cumulative proportion of the genomes contained in ROH below the length displayed on the x axis. Thin lines represent individual genomes, whereas thick lines show population averages. Trajectories of modern and historical genomes start diverging at long ROH (>1 Mb).

See also Figures S1–S3.

century (Figure 3B). Finally, we predicted the possible deleterious impact of each amino acid substitution on the protein function using physical considerations [18]. We observed a significant increase in the frequency of amino acid substitutions classified as "probably damaging" in the modern Grauer's gorilla individuals, whereas no significant change was observed between historical and modern mountain gorillas (Figure 3C).

Genes affected by LoF mutations with the highest frequency increase in the modern Grauer's gorillas were associated with functions related to immunity and methylation (see Data S2 and S3), possibly indicating a decline in pathogen resistance during recent decades. LoF variants with the highest frequency increase in modern mountain gorillas were enriched for genes related to Sertoli cell differentiation, thus possibly affecting male fertility (see Data S2 and S3). In addition, both Grauer's and mountain gorillas show several high-frequency LoF variants that are related to malformation of fingers and toes, corroborating the reports of syndactyly in eastern gorillas (see Data S3) [19].

By analyzing complete genomes from museum-preserved historical specimens, we have identified and quantified the genomic consequences of population decline in eastern gorillas during the last century. Comparisons to the modern western lowland gorillas (estimated population size: 360,000 individuals), which diverged from the eastern gorillas around 150,000 years ago [12, 20], demonstrate that differences in genetic diversity between species are dominated by long-term demographic processes. The observed decrease in genome-wide diversity and increase in putatively deleterious variants in eastern gorillas (Figures 2 and 3) is striking given the short time period spanned by our study, corresponding to 4–5 gorilla generations. Grauer's gorillas have been more severely affected than mountain gorillas, which we hypothesize can be attributed to their contrasting demographic histories.

Eastern gorillas experienced continuous population decline for the last 100,000 years [12], before diverging into Grauer's and mountain gorillas, ca. 10,000 years ago [21]. Subsequently, Grauer's gorillas went through a period of population growth and range expansion 5,000–10,000 years ago [22, 23]. This demographic expansion may have led not only to a historically higher genetic diversity in Grauer's compared to mountain gorillas (Figure 2) but also to a higher number of low-frequency deleterious mutations in the Grauer's gorilla population [24, 25]. As Grauer's gorillas went through a severe population decline of 80% in the last 20 years to less than 4,000 individuals today [26], these deleterious mutations appear to have increased in frequency, likely due to increased drift and inbreeding (Figure 2), thus leading to a more pronounced change in genetic load in Grauer's compared to mountain gorillas (Figure 3). In contrast, the population size of mountain gorillas from the Virunga Massif population has likely remained small since their divergence from the Grauer's gorillas [22, 23]. Numbering fewer than 1,000 individuals at least since the late 1950s [27], mountain gorillas experienced a population low of ~250 individuals in the 1980s [28] but recovered to ~450 individuals in 2013 [29]. However, we do not detect significant differences in genetic diversity, inbreeding, and genetic load between historical and modern mountain gorilla samples. This might be due to both purging of genetic load as a result of the continuously small population size in mountain gorillas during the last 10,000 years as well as the rapid population recovery in recent decades thanks

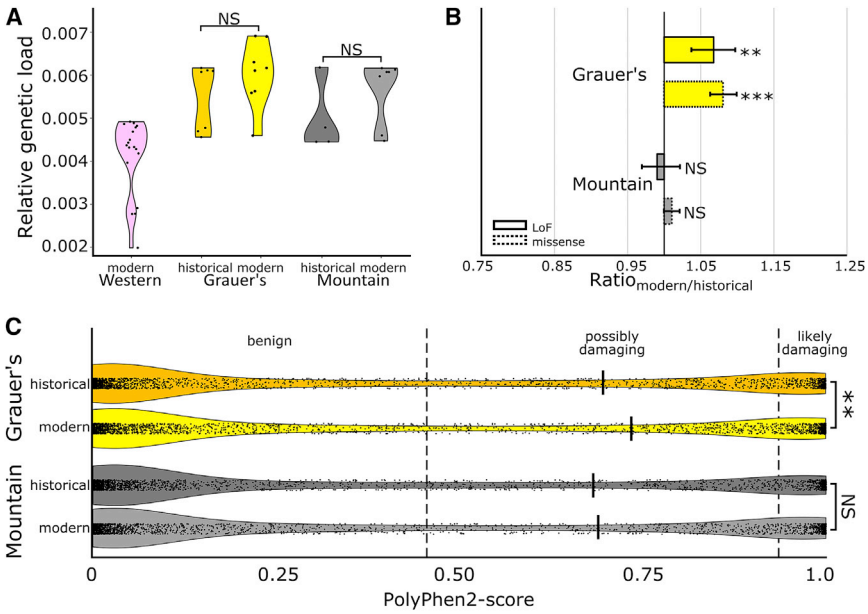

Figure 3. Functional Consequences of Population Decline in Eastern Gorillas

(A) Relative genetic load measured as the fraction of homozygous-derived sites in evolutionary-constrained regions of the genome.

(B) Ratio of derived alleles between historical and modern genomes at LoF and missense sites. Error bars, ±1 SD. This ratio is significantly different from 1 in Grauer's gorillas.

(C) The likelihood of an amino acid substitution being damaging for homozygous variants within eastern gorilla populations. Solid lines show population averages for all alleles classified as possible and likely damaging (PolyPhen2 score > 0.45).

**p < 0.01, ***p < 0.001; NS, not significant. See also Figures S2 and S3.

to implemented conservation measures and/or a less pronounced population decline than previously reported [28, 30].

Many species have experienced severe population declines in the last centuries [2] and may thus face similar genomic consequences as reported here for Grauer's gorillas. In species with shorter generation time, such consequences may be even more severe due to faster genomic change. Nevertheless, if population declines occur more gradually or bottlenecks are short-lived and followed by population recovery within only a few generations, species are likely to be less impacted by negative genomic consequences, as exemplified by the mountain gorillas.

STAR★METHODS

Detailed methods are provided in the online version of this paper and include the following:

- KEY RESOURCES TABLE
- CONTACT FOR REAGENT AND RESOURCE SHARING
- EXPERIMENTAL MODEL AND SUBJECT DETAILS
- METHOD DETAILS
  - DNA extraction, library preparation and sequencing
  - Read mapping, post-mortem DNA damage, SNP calling and filtering
  - Post mortem DNA damage in historical genomes
  - Genotype likelihood and SNP calling
  - PCA and Admixture
  - Heterozygosity and nucleotide diversity
  - Runs of homozygosity
  - Genetic load
- DATA AND SOFTWARE AVAILABILITY

SUPPLEMENTAL INFORMATION

Supplemental Information includes three figures and three data files and can be found with this article online at https://doi.org/10.1016/j.cub.2018.11.055.

ACKNOWLEDGMENTS

We thank Emmanuel Gilissen, Patrick Semal, Daniela C. Kalthoff, Gontran Sonet, Isabel Ordaz Németh, and Zoltan T. Nagy for their support during the study of natural history collections and Matthias Meyer for helpful discussions. Sequencing was performed by the Swedish National Genomics Infrastructure (NGI) at the Science for Life Laboratory, which is supported by the Swedish Research Council and the Knut and Alice Wallenberg Foundation. The authors acknowledge support from the Uppsala Multidisciplinary Centre for Advanced Computational Science for assistance with massively parallel sequencing and access to the UPPMAX computational infrastructure. This research was supported by BFU2017-86471-P (MINECO/FEDER, UE), U01 MH106874 grant, Howard Hughes International Early Career, Obra Social "La Caixa" and Secretaria d'Universitats i Recerca and CERCA Programme del Departament d'Economia i Coneixement de la Generalitat de Catalunya (GRC 2017 SGR 880) to T.M.-B., the Human Frontier Science Program Postdoctoral Fellowship (LT000800/2011-L), the Jan Löfqvist and the Nilsson-Ehle Endowments of the Royal Physiographic Society in Lund, FORMAS (2016-00835) to K.G., and FORMAS (2015-676) to L.D.

AUTHOR CONTRIBUTIONS

Conceptualization, T.v.d.V., L.D., and K.G.; Methodology, T.v.d.V., D.D.-d.-M., T.M.-B., K.G., and L.D.; Investigation, T.v.d.V., D.D.-d.-M.; Writing, T.v.d.V. and K.G. with input from all co-authors; Funding Acquisition, L.D. and K.G.; Resources, L.D. and K.G.; Supervision, L.D. and K.G.

DECLARATION OF INTERESTS

The authors declare no competing interests.

Received: September 12, 2018
Revised: November 12, 2018
Accepted: November 21, 2018
Published: December 27, 2018

REFERENCES

1. Waters, C.N., Zalasiewicz, J., Summerhayes, C., Barnosky, A.D., Poirier, C., Gałuszka, A., Cearreta, A., Edgeworth, M., Ellis, E.C., Ellis, M., et al. (2016). The Anthropocene is functionally and stratigraphically distinct from the Holocene. Science *351*, aad2622.

2. Pimm, S.L., Jenkins, C.N., Abell, R., Brooks, T.M., Gittleman, J.L., Joppa, L.N., Raven, P.H., Roberts, C.M., and Sexton, J.O. (2014). The biodiversity of species and their rates of extinction, distribution, and protection. Science *344*, 1246752.
3. Lande, R. (1993). Risks of Population Extinction from Demographic and Environmental Stochasticity and Random Catastrophes. Am. Nat. *142*, 911–927.
4. Reed, D.H., and Frankham, R. (2003). Correlation between fitness and genetic diversity. Conserv. Biol. *17*, 230–237.
5. Lande, R., and Shannon, S. (1996). The Role of Genetic Variation in Adaptation and Population Persistence in a Changing Environment. Evolution *50*, 434–437.
6. Keller, L.F., and Waller, D.M. (2002). Inbreeding effects in wild populations. Trends Ecol. Evol. *17*, 230–241.
7. Lande, R. (1988). Genetics and demography in biological conservation. Science *241*, 1455–1460.
8. Smith, K.F., Sax, D.F., and Lafferty, K.D. (2006). Evidence for the role of infectious disease in species extinction and endangerment. Conserv. Biol. *20*, 1349–1357.
9. Díez-del-Molino, D., Sánchez-Barreiro, F., Barnes, I., Gilbert, M.T.P., and Dalén, L. (2018). Quantifying Temporal Genomic Erosion in Endangered Species. Trends Ecol. Evol. *33*, 176–185.
10. IUCN (2017). The IUCN Red List of Threatened Species. Version 2017.3.
11. Prado-Martinez, J., Sudmant, P.H., Kidd, J.M., Li, H., Kelley, J.L., Lorente-Galdos, B., Veeramah, K.R., Woerner, A.E., O'Connor, T.D., Santpere, G., et al. (2013). Great ape genetic diversity and population history. Nature *499*, 471–475.
12. Xue, Y., Prado-Martinez, J., Sudmant, P.H., Narasimhan, V., Ayub, Q., Szpak, M., Frandsen, P., Chen, Y., Yngvadottir, B., Cooper, D.N., et al. (2015). Mountain gorilla genomes reveal the impact of long-term population decline and inbreeding. Science *348*, 242–245.
13. Gordon, D., Huddleston, J., Chaisson, M.J.P., Hill, C.M., Kronenberg, Z.N., Munson, K.M., Malig, M., Raja, A., Fiddes, I., Hillier, L.W., et al. (2016). Long-read sequence assembly of the gorilla genome. Science *352*, aae0344.
14. Sawyer, S., Krause, J., Guschanski, K., Savolainen, V., and Pääbo, S. (2012). Temporal patterns of nucleotide misincorporations and DNA fragmentation in ancient DNA. PLoS ONE *7*, e34131.
15. Korneliussen, T.S., Albrechtsen, A., and Nielsen, R. (2014). ANGSD: Analysis of Next Generation Sequencing Data. BMC Bioinformatics *15*, 356.
16. Kardos, M., Åkesson, M., Fountain, T., Flagstad, Ø., Liberg, O., Olason, P., Sand, H., Wabakken, P., Wikenros, C., and Ellegren, H. (2018). Genomic consequences of intensive inbreeding in an isolated wolf population. Nat Ecol Evol *2*, 124–131.
17. Pollard, K.S., Hubisz, M.J., Rosenbloom, K.R., and Siepel, A. (2010). Detection of nonneutral substitution rates on mammalian phylogenies. Genome Res. *20*, 110–121.
18. Adzhubei, I., Jordan, D.M., and Sunyaev, S.R. (2013). Predicting functional effect of human missense mutations using PolyPhen-2. Curr. Protoc. Hum. Genet. Chapter 7: Unit 7.20.
19. Mudakikwa, A., Cranfield, M.R., Sleeman, J.M., and Eilenberger, U. (2005). Clinical medicine, preventive health care and research on mountain gorillas in the Virunga Volcanoes region. In Mountain Gorillas : Three decades of research at Karisoke, M.M. Robbins, P. Sicotte, and K.J. Stewart, eds. (Cambridge: Cambridge University Press), pp. 342–360.
20. Strindberg, S., Maisels, F., Williamson, E.A., Blake, S., Stokes, E.J., Aba'a, R., Abitsi, G., Agbor, A., Ambahe, R.D., Bakabana, P.C., et al. (2018). Guns, germs, and trees determine density and distribution of gorillas and chimpanzees in Western Equatorial Africa. Sci. Adv. *4*, eaar2964.
21. Roy, J., Arandjelovic, M., Bradley, B.J., Guschanski, K., Stephens, C.R., Bucknell, D., Cirhuza, H., Kusamba, C., Kyungu, J.C., Smith, V., et al. (2014). Recent divergences and size decreases of eastern gorilla populations. Biol. Lett. *10*, 20140811.
22. Tocheri, M.W., Dommain, R., McFarlin, S.C., Burnett, S.E., Troy Case, D., Orr, C.M., Roach, N.T., Villmoare, B., Eriksen, A.B., Kalthoff, D.C., et al. (2016). The evolutionary origin and population history of the grauer gorilla. Am. J. Phys. Anthropol. *159* (*Suppl 61*), S4–S18.
23. van der Valk, T., Sandoval-Castellanos, E., Caillaud, D., Ngobobo, U., Binyinyi, E., Nishuli, R., Stoinski, T., Gilissen, E., Sonet, G., Semal, P., et al. (2018). Significant loss of mitochondrial diversity within the last century due to extinction of peripheral populations in eastern gorillas. Sci. Rep. *8*, 6551.
24. Gazave, E., Chang, D., Clark, A.G., and Keinan, A. (2013). Population growth inflates the per-individual number of deleterious mutations and reduces their mean effect. Genetics *195*, 969–978.
25. Peischl, S., and Excoffier, L. (2015). Expansion load: recessive mutations and the role of standing genetic variation. Mol. Ecol. *24*, 2084–2094.
26. Plumptre, A.J., Nixon, S., Kujirakwinja, D.K., Vieilledent, G., Critchlow, R., Williamson, E.A., Nishuli, R., Kirkby, A.E., and Hall, J.S. (2016). Catastrophic Decline of World's Largest Primate: 80% Loss of Grauer's Gorilla (Gorilla beringei graueri) Population Justifies Critically Endangered Status. PLoS ONE *11*, e0162697.
27. Harcourt, A.H., and Fossey, D. (1981). The Virunga gorillas: decline of an 'island' population. Afr. J. Ecol. *19*, 83–97.
28. Kalpers, J., Williamson, E.A., Robbins, M.M., McNeilage, A., Nzamurambaho, A., Lola, N., and Mugiri, G. (2003). Gorillas in the crossfire: population dynamics of the Virunga mountain gorillas over the past three decades. Oryx *37*, 326–337.
29. Gray, M., Roy, J., Vigilant, L., Fawcett, K., Basabose, A., Cranfield, M., Uwingeli, P., Mburanumwe, I., Kagoda, E., and Robbins, M.M. (2013). Genetic census reveals increased but uneven growth of a critically endangered mountain gorilla population. Biol. Conserv. *158*, 230–238.
30. Robbins, M.M., Gray, M., Fawcett, K.A., Nutter, F.B., Uwingeli, P., Mburanumwe, I., Kagoda, E., Basabose, A., Stoinski, T.S., Cranfield, M.R., et al. (2011). Extreme conservation leads to recovery of the Virunga mountain gorillas. PLoS ONE *6*, e19788.
31. Rohland, N., and Reich, D. (2012). Cost-effective, high-throughput DNA sequencing libraries for multiplexed target capture. Genome Res. *22*, 939–946.
32. Meyer, M., and Kircher, M. (2010). Illumina sequencing library preparation for highly multiplexed target capture and sequencing. Cold Spring Harb. Protoc. https://doi.org/10.1101/pdb.prot5448.
33. Schubert, M., Lindgreen, S., and Orlando, L. (2016). AdapterRemoval v2: rapid adapter trimming, identification, and read merging. BMC Res. Notes *9*, 88.
34. Li, H., and Durbin, R. (2009). Fast and accurate short read alignment with Burrows-Wheeler transform. Bioinformatics *25*, 1754–1760.
35. McKenna, A., Hanna, M., Banks, E., Sivachenko, A., Cibulskis, K., Kernytsky, A., Garimella, K., Altshuler, D., Gabriel, S., Daly, M., and DePristo, M.A. (2010). The Genome Analysis Toolkit: a MapReduce framework for analyzing next-generation DNA sequencing data. Genome Res. *20*, 1297–1303.
36. Danecek, P., Auton, A., Abecasis, G., Albers, C.A., Banks, E., DePristo, M.A., Handsaker, R.E., Lunter, G., Marth, G.T., Sherry, S.T., et al.; 1000 Genomes Project Analysis Group (2011). The variant call format and VCFtools. Bioinformatics *27*, 2156–2158.
37. Jónsson, H., Ginolhac, A., Schubert, M., Johnson, P.L.F., and Orlando, L. (2013). mapDamage2.0: fast approximate Bayesian estimates of ancient DNA damage parameters. Bioinformatics *29*, 1682–1684.
38. Quinlan, A.R., and Hall, I.M. (2010). BEDTools: a flexible suite of utilities for comparing genomic features. Bioinformatics *26*, 841–842.
39. Bolger, A.M., Lohse, M., and Usadel, B. (2014). Trimmomatic: a flexible trimmer for Illumina sequence data. Bioinformatics *30*, 2114–2120.
40. Li, H., Handsaker, B., Wysoker, A., Fennell, T., Ruan, J., Homer, N., Marth, G., Abecasis, G., and Durbin, R.; 1000 Genome Project Data Processing Subgroup (2009). The Sequence Alignment/Map format and SAMtools. Bioinformatics *25*, 2078–2079.

41. Derrien, T., Estellé, J., Marco Sola, S., Knowles, D.G., Raineri, E., Guigó, R., and Ribeca, P. (2012). Fast computation and applications of genome mappability. PLoS ONE *7*, e30377.

42. Narasimhan, V., Danecek, P., Scally, A., Xue, Y., Tyler-Smith, C., and Durbin, R. (2016). BCFtools/RoH: a hidden Markov model approach for detecting autozygosity from next-generation sequencing data. Bioinformatics *32*, 1749–1751.

43. McLaren, W., Gil, L., Hunt, S.E., Riat, H.S., Ritchie, G.R.S., Thormann, A., Flicek, P., and Cunningham, F. (2016). The Ensembl Variant Effect Predictor. Genome Biol. *17*, 122.

44. Eden, E., Navon, R., Steinfeld, I., Lipson, D., and Yakhini, Z. (2009). GOrilla: a tool for discovery and visualization of enriched GO terms in ranked gene lists. BMC Bioinformatics *10*, 48.

45. Dabney, J., Knapp, M., Glocke, I., Gansauge, M.-T., Weihmann, A., Nickel, B., Valdiosera, C., García, N., Pääbo, S., Arsuaga, J.-L., and Meyer, M. (2013). Complete mitochondrial genome sequence of a Middle Pleistocene cave bear reconstructed from ultrashort DNA fragments. Proc. Natl. Acad. Sci. USA *110*, 15758–15763.

46. Ersmark, E., Orlando, L., Sandoval-Castellanos, E., Barnes, I., Barnett, R., Stuart, A., Lister, A., and Dalén, L. (2015). Population Demography and Genetic Diversity in the Pleistocene Cave Lion. Open Quat. *1*, 1–15.

47. van der Valk, T., Lona Durazo, F., Dalén, L., and Guschanski, K. (2017). Whole mitochondrial genome capture from faecal samples and museum-preserved specimens. Mol. Ecol. Resour. *17*, e111–e121.

48. Li, H. (2013). Aligning sequence reads, clone sequences and assembly contigs with BWA-MEM. arXiv, arXiv:1303.3997, https://arxiv.org/abs/1303.3997.

49. Briggs, A.W., Stenzel, U., Meyer, M., Krause, J., Kircher, M., and Pääbo, S. (2010). Removal of deaminated cytosines and detection of in vivo methylation in ancient DNA. Nucleic Acids Res. *38*, e87.

50. Nielsen, R., Paul, J.S., Albrechtsen, A., and Song, Y.S. (2011). Genotype and SNP calling from next-generation sequencing data. Nat. Rev. Genet. *12*, 443–451.

51. DePristo, M.A., Banks, E., Poplin, R., Garimella, K.V., Maguire, J.R., Hartl, C., Philippakis, A.A., del Angel, G., Rivas, M.A., Hanna, M., et al. (2011). A framework for variation discovery and genotyping using next-generation DNA sequencing data. Nat. Genet. *43*, 491–498.

52. Li, H. (2014). Toward better understanding of artifacts in variant calling from high-coverage samples. Bioinformatics *30*, 2843–2851.

53. Fumagalli, M., Vieira, F.G., Korneliussen, T.S., Linderoth, T., Huerta-Sánchez, E., Albrechtsen, A., and Nielsen, R. (2013). Quantifying population genetic differentiation from next-generation sequencing data. Genetics *195*, 979–992.

54. Skotte, L., Korneliussen, T.S., and Albrechtsen, A. (2013). Estimating individual admixture proportions from next generation sequencing data. Genetics *195*, 693–702.

55. Nielsen, R., Korneliussen, T., Albrechtsen, A., Li, Y., and Wang, J. (2012). SNP calling, genotype calling, and sample allele frequency estimation from New-Generation Sequencing data. PLoS ONE *7*, e37558.

56. Thompson, E.A. (2013). Identity by descent: variation in meiosis, across genomes, and in populations. Genetics *194*, 301–326.

57. Henn, B.M., Botigué, L.R., Bustamante, C.D., Clark, A.G., and Gravel, S. (2015). Estimating the mutation load in human genomes. Nat. Rev. Genet. *16*, 333–343.

58. Cooper, G.M., and Shendure, J. (2011). Needles in stacks of needles: finding disease-causal variants in a wealth of genomic data. Nat. Rev. Genet. *12*, 628–640.

59. Librado, P., Gamba, C., Gaunitz, C., Der Sarkissian, C., Pruvost, M., Albrechtsen, A., Fages, A., Khan, N., Schubert, M., Jagannathan, V., et al. (2017). Ancient genomic changes associated with domestication of the horse. Science *356*, 442–445.

STAR★METHODS

KEY RESOURCES TABLE

REAGENT or RESOURCE	SOURCE	IDENTIFIER
Chemicals, Peptides, and Recombinant Proteins		
Tango Buffer	Thermofisher Scientific	Cat#: BY5
dNTP's	Thermofisher Scientific	Cat#: R1121
ATP	Thermofisher Scientific	Cat#: R0441
T4 PNK	Thermofisher Scientific	Cat#: EK0031
USER enzyme	NEB	Cat#: M5505S
T4 DNA ligase Buffer	Thermofisher Scientific	Cat#: EL0014
T4 DNA Polymerase	Thermofisher Scientific	Cat#: EP0061
PEG-4000	Merck	Cat#: 25322-68-3
T4 DNA ligase	Thermofisher Scientific	Cat#: EL0014
Isothermal Amplification buffer	New England Biolabs	Cat#: B0537S
Bst polymerase 2.0, Large Fragment	New England Biolabs	Cat#: M0275S
Pfu Turbo Cx Hotstart DNA Buffer	Agilent technologies	Cat#: 600410
Pfu Turbo Cx Hotstart DNA Polymerase	Agilent technologies	Cat#: 600410
TritonX	Merck	Cat#: 600410
Proteinase K	Sigma	Cat#: 9002-93-1
EDTA	Thermofisher Scientific	Cat#: 15575020
Guanidine hydrochloride	Sigma	Cat#: G3272-500G
Tween-20	Sigma	Cat#: P9416-50ML
Isopropanol	Sigma	Cat#: 650447
Tris-HCl	Thermofisher Scientific	Cat#: AM9855G
Critical Commercial Assays		
High Pure Viral Nucleic Acid Large Volume Kit	Roche	Cat#: 05114403001
MinElute PCR Purification Kit	QIAGEN	Cat#: 28004
AMPure XP Beads	Agencourt	Cat#: A63881
Deposited Data		
Raw and analyzed data	This paper	ENA: PRJEB29503
Gorilla reference genome	[13]	ftp://ftp.ncbi.nlm.nih.gov/genomes/all/GCF/000/151/905/GCF_000151905.2_gorGor4
Gorilla whole genome resequencing data	[11]	https://www.ncbi.nlm.nih.gov/bioproject/189439
Gorilla whole genome resequencing data	[12]	https://www.ebi.ac.uk/ena/data/view/PRJEB3220
Base-wise phyloP scores	[17]	ftp://hgdownload.cse.ucsc.edu/goldenPath/mm9/phyloP30way/placentalMammals/
hg38ToGorGor4 chainfile	N/A	http://hgdownload.cse.ucsc.edu/gbdb/hg38/liftOver/
Experiment models: Organism		
38 *Gorilla beringei graueri* museum specimens (teeth and skin)	Royal Museum for Central Africa (Tervuren, Belgium) and Royal Belgian Institute of Natural Sciences (Brussels, Belgium)	See Data S1
21 *Gorilla beringei beringei* museum specimens (teeth)	Swedish Museum of Natural History (Stockholm, Sweden)	See Data S1
Oligonucleotides		
Barcode-primer1: 5′ -> 3′ CTTTCCCTACACGACGCTCTTCCGATCTatcgatt	CytoGene	[31]

(*Continued on next page*)

Continued

REAGENT or RESOURCE	SOURCE	IDENTIFIER
Barcode-primer2: 5′ -> 3′ CTTTCCCTACACGACGCTCTTCCG ATCTaacgcta	CytoGene	[31]
Barcode-primer3: 5′ -> 3′ CTTTCCCTACACGACGCTCTTCCG ATCTggtatcg	CytoGene	[31]
Barcode-primer4: 5′ -> 3′ CTTTCCCTACACGACGCTCTTCCG ATCTtgactgg	CytoGene	[31]
Barcode-primer5: 5′ -> 3′ CTTTCCCTACACGACGCTCTTCCG ATCTcaattgc	CytoGene	[31]
Barcode-primer6: 5′ -> 3′ CTTTCCCTACACGACGCTCTTCCG ATCTtggccat	CytoGene	[31]
IS5_reamp.P5: 5′ -> 3′ AATGATACGGCGACCACCGA	CytoGene	[32]
IS6_reamp.P7: 5′ -> 3′ CAAGCAGAAGACGGCATACGA	CytoGene	[32]
Pre_Hyb_F: 5′ -> 3′ CTTTCCCTACACGACGCTCTTC	CytoGene	[31]
Pre_Hyb_R: 5′ -> 3′ GTGACTGGAGTTCAGACGTGTGCT	CytoGene	[31]
P7 index and sequencing-primer: 5′ -> 3′ AAGCAGAAGACGGCATACGAGAT gaagattGTGACTGGAGTTCAGACGTGT	CytoGene	[32]
P5 sequencing-primer: 5′ -> 3′ AAGCAGAAGACGGCATACGAGATG TGACTGGAGTTCAGACGTGT	CytoGene	[32]
Software and Algorithms		
AdapterRemovalV2	[33]	https://github.com/MikkelSchubert/adapterremoval/; RRID: SCR_011834
BWA	[34]	http://bio-bwa.sourceforge.net/; RRID: SCR_010910
GATK v3.8	[35]	https://software.broadinstitute.org/gatk/; RRID: SCR_001876
Picard	N/A	https://broadinstitute.github.io/picard/; RRID: SCR_006525
Vcftools	[36]	https://vcftools.github.io/index.html; RRID: SCR_001235
MapDamage2.0	[37]	ginolhac.github.io/mapDamage/; RRID: SCR_001240
BEDTools	[38]	https://bedtools.readthedocs.io/en/latest/; RRID: SCR_006646
Trimmomatic	[39]	http://www.usadellab.org/cms/?page=trimmomatic; RRID: SCR_011848
SAMtools	[40]	http://samtools.sourceforge.net/; RRID: SCR_002105
Python 2.7	N/A	https://www.python.org/downloads/release/python-2715/; RRID: SCR_008394
R	N/A	https://www.r-project.org/; RRID: SCR_001905
ANGSD	[15]	https://github.com/ANGSD/angsd
GEM	[41]	http://gemlibrary.sourceforge.net
htsbox	N/A	https://github.com/lh3/htsbox

(*Continued on next page*)

Continued

REAGENT or RESOURCE	SOURCE	IDENTIFIER
bcftools	[42]	http://www.htslib.org/doc/bcftools.html; RRID: SCR_005227
liftOver	N/A	https://genome.sph.umich.edu/wiki/LiftOver; RRID: SCR_001173
Ensembl Variant Effect Predictor	[43]	https://www.ensembl.org/info/docs/tools/vep/index.html; RRID: SCR_007931
PolyPhen-2	[18]	http://genetics.bwh.harvard.edu/pph2/; RRID: SCR_013189
GOrilla	[44]	http://cbl-gorilla.cs.technion.ac.il/; RRID: SCR_006848

CONTACT FOR REAGENT AND RESOURCE SHARING

Further information and requests for resources and reagents should be directed to and will be fulfilled by the Lead Contact, Katerina Guschanski (katerina.guschanski@ebc.uu.se).

EXPERIMENTAL MODEL AND SUBJECT DETAILS

Historical Grauer's gorilla samples (n = 38) with age ranging from 108 – 32 years (median year of collection = 1949) were collected at the Royal Belgian Institute of Natural Sciences (RBINS) in Brussels and the Royal Museum for Central Africa (RMCA) in Tervuren, Belgium. Historical mountain gorilla samples from the Virunga Massif population (n = 21) with age ranging from 104 – 61 years (median year of collection = 1921) were obtained from the Swedish Museum of Natural History (NRM) in Stockholm.

METHOD DETAILS

DNA extraction, library preparation and sequencing

DNA from historical samples, consisting of teeth and dried soft-tissue samples, was extracted in dedicated ancient DNA facilities at Uppsala University, Uppsala, and the Swedish Museum of Natural History, Stockholm. Surface contamination from teeth was removed by exposing the roots to UV light (245 nm) for 10 min, abrading the surface with an engraving cutter using a Dremel 8100 drill, and again subjecting the cleaned surfaces to UV light for 10 min. No surface decontamination was performed for soft-tissue samples. The Grauer's gorilla samples were extracted using an extraction protocol optimized for retention of short fragments in ancient DNA samples [45]. Mountain gorilla samples were extracted with Vivapsin filters as in *Ersmark et. al.* [46]. For screening, we prepared pooled Illumina sequencing libraries from all mountain and Grauer's gorilla DNA extracts following the strategy outlined in [31] and [47]. Briefly, 20 μL of DNA extract was used in a 40 μL blunting reaction (final concentrations: 1 × buffer Tango, 100 μM each dNTP, 1 mM ATP, 25 U T4 polynucleotide kinase (Thermo Scientific), 5U T4 DNA polymerase (Thermo Scientific)). Samples were incubated at 25°C for 15 min followed by 5 min at 12°C. DNA fragments within each sample were then ligated to a combination of incomplete, partially double-stranded P5- and P7-adapters (10 μM each), each containing a unique seven base pair sequence, referred to as barcode. Adapter ligation was performed in a 40 μL reaction volume using 20 μL of blunted DNA and 1 μL of unique P5 and P7 barcoded adapters per sample (final concentrations: 1 × T4 DNA ligase buffer, 5% PEG-4000, 5U T4 DNA ligase (Thermo Scientific)). Samples were incubated for 30 min at room temperature and cleaned using MinElute spin columns following the manufacturer's protocol. Adapter fill-in was performed in 40 μL final volume using 20 μL adapter ligated DNA (final concentrations: 1 × T4 DNA ligase buffer, 5% PEG-4000, 5 U T4 DNA ligase (Thermo Scientific)), incubated at 37°C for 20 min, heat-inactivated at 80°C for 20 min, and cleaned using MinElute spin columns, as above. For the purpose of shallow shotgun sequencing, indexing PCR was performed for 10 cycles in 25 μL reaction volume (3 μL of adapter-ligated library as input) using a unique P7 indexing primer for each sample, as in *Meyer & Kircher (2010)* [32] (final concentrations: 1x AccuPrime reaction mix, 0.3 μM IS4 primer, 0.3 μM P7 indexing primer, 7 U AccuPrime Pfx (Thermo Scientific), cycling protocol: 95°C for 2 min, 10 cycles at 95°C for 30 s, 55°C for 30 s and 72°C for 1 min and a final extension at 72°C for 5 min). Sample libraries were cleaned using MinElute spin columns and subsequently fragment length distribution and concentration were measured on the Bioanalyzer. Samples were pooled in equimolar amounts into two final library pools and size selected with two rounds of AMPure XP bead clean-up, using 0.5X and 1.8X bead:DNA ratio, respectively. Both library pools with final concentration of 10nM were subjected to 125 bp paired-end shotgun sequencing on the Illumina HiSeq 2500 platform (one lane each, High Output Mode) at the SciLifeLab sequencing facility in Stockholm. Samples were demultiplexed based on their unique indices using bcl2fastq v2.17.1 with default settings (Illumina Inc.). We removed adapter sequences, including barcodes, and used AdapterRemovalV2 [33] with default parameters to collapse and remove reads shorter than 15 base pairs. Collapsed reads were mapped against the gorilla reference genome (gorGor4) [13] using bwa-mem with default parameters [48]. We then estimated the endogenous content for each sample as the fraction of reads mapping to the reference genome with a quality

score > 20 (Phred-scale) (see Data S1). Note that we did not remove duplicate reads at this stage, since duplicate removal tools (samtools rmdup and Picard MarkDuplicates) only remove duplicates among the mapped reads, biasing the endogenous content estimates. Post-mortem DNA damage patterns were identified using mapDamage2.0 [37]. We also assessed human contamination as in *van der Valk et al.* (2017) [47]. Briefly, we identified fixed nucleotide difference between a panel of mitochondrial genomes from nine human with diverse geographic origin [11] and 13 published eastern gorilla mitochondrial genomes [12]. For each of these diagnostic sites covered by at least three sequencing reads, we calculated the proportion of reads containing the human variant and averaged the estimate over all diagnostic sites (see Data S1).

After screening we selected seven Grauer's and four mountain gorilla samples displaying high endogenous content and low levels of human contamination for UDG treatment to remove post-mortem DNA damage and subsequent deep sequencing. Libraries were then prepared as above with slight modifications: During blunt end repair, 20 μL of DNA extract was used in a 50 μL reaction together with USER enzyme treatment to remove uracil bases resulting from post-mortem damage (final concentrations: 1 × buffer Tango, 100 μM each dNTP, 1 mM ATP, 25 U T4 polynucleotide kinase (Thermo Scientific), 3U USER enzyme (NEB)). Samples were incubated for 3 h at 37°C, followed by the addition of 1 μL T4 DNA polymerase (Thermo Scientific) and incubation at 25°C for 15 min and 12°C for 5 min. Indexing PCR for all adapter ligated libraries was performed as above for 10 cycles, but in 125 μL volume (18 μL of adapter ligated input DNA) and each of these samples was sequenced on one HiSeq X lane 150bp paired-end. Samples with insufficient coverage (n = 7) after deep-sequencing were pooled and sequenced on an additional five HiSeq X lanes.

Read mapping, post-mortem DNA damage, SNP calling and filtering

Pooled libraries were demultiplexed based on their unique 7bp barcodes (see Data S1) and we subsequently removed adapter and barcode sequences and collapsed fastq-reads by individual using AdapterRemovalV2 [33]. Collapsed reads were mapped against the western lowland gorilla reference genome with bwa-mem on default settings (including readgroups and marking shorter split hits as secondary for Picard compatibility) [48]. After mapping, alignments around indels were improved using GATKv3.8 indelRealigner [35]. We then removed duplicate reads using Picard (https://broadinstitute.github.io/picard/). We estimated remaining levels of post-mortem DNA damage (note that the libraries were UDG-treated) and rescaled mapping quality scores to correct for any remaining damage using Mapdamage2.0 on default parameters [37]. After quality score rescaling, we filtered out all reads below mapping quality of 20 (Phred-scale) and removed sex chromosomes from further analyses.

Raw fastq files from published genomes of wild-born gorillas (17 western lowland, 7 mountain, and 8 Grauer's gorillas) were obtained from the European nucleotide archive (PRJNA189439 and PRJEB3220) [11, 12]. We removed sequencing adapters and subsequently bases at the start and end of the reads were trimmed if falling below the quality score of 15 (Phred33-scale) using Trimmomatic [39]. Read mapping, indel-realignment and duplicate removal was performed as above.

Post mortem DNA damage in historical genomes

All historical libraries were UDG-treated, removing the majority of post-mortem DNA damage [49]. We confirmed (using mapDamage2.0) that remaining typical ancient DNA post-mortem damage (C-to-T substitutions at read ends) in historical samples was present only at very low rates (Figure S1A). However UDG-treatment has lower efficiency of removing uracil nucleotides at CpG sites [49] and therefore remaining post-mortem DNA damage at these positions may cause biases in downstream analyses. We estimated the extent of damage at CpG sites as the fraction of mapped reads containing a thymine nucleotide at a cytosine position that is part of a CpG site. To this end, we first identified all CpG sites in the gorilla reference genome defined as sites where C is immediately followed by a G and used samtools mpileup to obtain all mapped bases with Q > 20 at each site per genome. We then quantified the fraction of thymine nucleotides at the identified CpG sites for each genome and averaged this fraction over all identified CpG sites within the genome (Figure S1B).

Genotype likelihood and SNP calling

Most of our analyses were conducted in a genotype likelihood framework implemented in the ANGSD software, allowing for the incorporation of statistical uncertainty in low-coverage data [15, 50]. Genotype likelihoods for all gorilla samples were calculated adjusting mapping quality for regions with excessive mismatches (-C 50), removing reads with multiple hits (-uniqueOnly 1), base quality score below 20 (-minQ 20), and downgrading quality scores around indels (-baq 1). We then only considered genotypes with a likelihood ratio test statistic of minimum 24 (-SNP_pval 2e-6) using the samtools genotype model (-GL 1).

SNPs were identified by creating a genomic VCF file for each individual using GATK UnifiedGenotyper with default parameters [35]. Subsequently, we used the GATK hard-filtering best-practice guideline for SNP-filtering [51]. Vcftools [36] was used to remove all sites with coverage depth below 3x, minimal allele count below 3, sites for which more than 75% of samples had a non-reference allele in a heterozygous state, indels, sites with higher than 3-fold average coverage across all individuals, and positions with SNP quality < 30 (Phred-scale), as recommended in [52]. Additionally, we removed all SNP within repetitive regions as identified with the GEM module [41]. Finally, we removed all SNPs at CpG sites, since these showed patterns of remaining post-mortem DNA damage (Figure S1B). We extensively assessed the effects of differential coverage between historical and modern genomes on population-level summary statistics by downsampling all modern genomes to similar coverage as the historical genomes (4X) using samtools V1.5 [40] and obtaining genotype-likelihoods for the downsampled genomes as described above. We observed slight biases on diversity estimates related to differential coverage (Figure S1C), and therefore all genomic comparisons were subsequently based on the modern genomes downsampled to 4X coverage.

PCA and Admixture

PCA plots were constructed using PCAngsd with default parameters and 200 EM iterations for computing the population allele frequencies [53]. To further explore genetic affinities and substructure in our data we used NGSadmix to estimate individual genome admixture proportions [54]. NGSadmix was run with the filtered genotype likelihoods and additional filtering of alleles below a frequency of 0.05 (-minMaf 0.05) (Figures S2A–S2E).

Heterozygosity and nucleotide diversity

We measured genome-wide heterozygosity using two different approaches. First, we estimated heterozygosity from the site frequency spectrum, obtained from the genotype-likelihoods with realSFS as implemented in ANGSD. We excluded transitions to eliminate possible biases from post-mortem DNA damage, such as those at CpG sites (Figures S1A and S1B), and performed 1000 bootstrap replicates for each sample to obtain confidence intervals (Figure S1C) [15, 55]. Second, we estimated genome-wide heterozygosity directly from the genomic VCF file (with down-sampled modern genomes and excluding CpG sites) by counting the proportion of heterozygous sites out of total sites covered by at least five reads in the filtered genomic VCF data (Figure S1D). In addition to estimating heterozygosity for each individual, we obtained population-level estimates of genetic diversity by calculating the number of divergent sites between individuals belonging to the same temporal population (treating historical and modern genomes of different gorilla taxa separately). To this end, we randomly sampled a single allele at each covered site excluding low quality bases (htsbox v1.0 -R -q 30 -Q 30 -l 35 -s 1, https://github.com/lh3/htsbox) within each individual genome. We then calculated the number of within population divergent sites in non-overlapping sliding windows of 10.000 base pairs, subsampling four random genomes for each window to eliminate the possibility that results are driven by differences in sample size between populations (Figure S1E).

We performed a permutation test to control for the possibility that the inferred differences in levels of genome-wide heterozygosity between modern and historical eastern gorillas could be driven by differences in sample size. For each dataset (i.e., VCF files of historical and modern genomes), we repeatedly (n = 1000) randomly subsampled four genomes (the smallest sample size in our analysis, equal to the number of historical mountain gorilla genomes), calculated genome-wide heterozygosity as described above, and assessed the significance of population level differences using pairwise t-tests in Scipy python package (v1.13.3). In 96.6% of randomization tests, the historical Grauer's gorilla populations shows significantly higher ($p < 0.05$) population level heterozygosity (Figure S2F), whereas none of the repeated 1000 comparisons were significant in mountain gorillas (p value > 0.05). Population structure in Grauer's gorillas (Figures 1B, S2A, and S2B) [12] could potentially explain the observed differences in heterozygosity between modern and historical samples. Although population structure was found in both modern and historical Grauer's gorillas, we performed an additional test to verify that it does not explain the observed decline in heterozygosity in this species. To this end, we estimated the average genome-wide heterozygosity based on the genomic VCF files within the larger Grauer's gorilla sub-cluster (popB) (Figure S2D), as it provided a large enough sample size for this analysis. Confirming our results at population level, heterozygosity was significantly higher ($p < 0.05$) in historical individuals in the sub-cluster popB compared to modern individuals from the same sub-cluster (Figure S2G). We then used the same approach as above to randomly subsample three historical and three modern individuals from popB (note three individuals is the lowest number required for significance testing) and found none of the tests resulted in higher heterozygosity in the modern dataset (Figure S2H).

Runs of homozygosity

To identify regions of the genome in complete homozygosity (runs of homozygosity, ROH), which are indicative of inbreeding, we applied a Hidden Markov Model (HMM) first described by Xue et al. (2015) [12] to the filtered SNP dataset assuming a constant recombination rate of 1×10^{-8} per base pair (Figure S3A). The emission probabilities in the HMM correspond to a Hardy-Weinberg model with inbreeding. Transition probabilities in the HMM incorporate the likelihood of a recombination event since the last site (see [42], for model details). The HMM model employed to infer ROH assigns confidence score to each of the genomic regions inferred to be in complete autozygosity. Even at relatively short ROH length (~100.000bp), the majority of such regions have a high confidence score (Figure S3B). This method thus allows for identification of genome stretches in complete homozygosity despite medium to low coverage. However, applying the model to low coverage genomes leads to a slight over-estimation of the number and length of homozygous tracts (Figure S3C), particularly for long ROH (> 2.5Mbp) (Figure S3D). Therefore, we controlled for differential coverage by down-sampling the modern genomes to 4x coverage as described above, before carrying out the comparisons of the distribution of ROH between historical and modern data (Figures 2B and 2C).

Runs of homozygosity arise when identical haplotypes are inherited from both parents. Over time these runs are broken apart by recombination events. Therefore, long runs of homozgyosity represent recent inbreeding events, whereas shorter runs stem from more ancient processes or mating between distant relatives. The largest difference between historical and modern genomes stems from ROH that are 5-6 Mb in length (Figure 2C). We estimate the mean number of generations back to the common ancestor of these homologous sequences using the formula from [56];

$$g = 100/2 \cdot ROH_{length}$$

where g is the number of generations (exponentially distributed) and ROH_{length} the ROH length in centimorgans. We use the physical length of ROH as approximation for the genetic length and estimate that ROH of 5-6 Mb trace back to less < 10 generations ago.

Genetic load

Estimating an individual's genetic load based on genomic data is challenging [57]. However, using evolutionary constraints as predictor for the fitness consequences of a mutation can serve as an approximation [58]. We therefore measured genetic load in each individual as the number of homozygous derived alleles in sites that are under strict evolutionary constraints divided by the total number of homozygous alleles, following the approach by Librado et al. (2017) [59] (Figure 3A).

Base-wise phyloP scores, pre-calculated for a whole-genome alignment of 20 mammals were obtained from Ensembl (Release 90). These scores show high accuracy in measuring regions of the genome under evolutionary constraints [17]. We converted the human genomic coordinates of the phyloP scores to the gorilla reference genome using the command-line version of the liftOver tool (https://genome-store.ucsc.edu/) and the hg38ToGorGor4 chainfile available from UCSC (http://hgdownload.cse.ucsc.edu/goldenPath/hg38/liftOver/). All sites with phyloP scores < 1, indicating low mammalian sequence conservation, were excluded. We considered only homozygous sites, since estimating the genetic load at heterozygous positions requires additional assumptions about the dominance coefficient of mutations. Using the genotype likelihood data, we then defined the genetic load (phyloPi) as the phyloP score at each given position multiplied by the probability of observing a derived homozygous allele (Pi) divided by the total number of homozygous sites in a given individual (hom).

To identify loss-of-function (LoF) and missense mutations in each gorilla individual (Figure 3B), we used the Ensembl Variant Effect Predictor (VEP) tool [43], which predicts the consequences of genomic variants on the protein sequence. Annotation of genes and transcripts for the gorilla reference genome (gorGor4) assembly were retrieved from the Ensembl VEP database (release 91, ftp://ftp.ensembl.org/pub/current_variation/VEP/). We used VEP to obtain classification for each of the SNPs in the filtered SNP dataset and subsequently classified SNPs into LoF, missense, and synonymous variants as in Xue et al. (2015):

- *LoF variants*: transcript_ablation, splice_donor_variant, splice_acceptor_variant, stop_gained, frameshift_variant, inframe_insertion, inframe_deletion, splice_region_variant
- *Missense variants*: missense_variant
- *Synonymous variants*: synonymous_variant

We compared the frequency of LoF variants between historical and modern data following the strategy outlined in Xue et al. (2015). Briefly, for each category of variants, we calculated at each site *i* the observed allele frequency in Population A as $f^A_i = d^A_i / n^A_i$, where n^A_i is the total number of alleles called in population A and d^A_i is the total number of called derived alleles. Similarly, we define f^B_i for population B. Then, if *C* is a category of protein-coding sites:

$$L_{A,B}(C) = \sum_{i \in C} f_i^A \left(1 - f_i^B\right)$$

We then calculate the ratio $R_{A/B(C)} = L_{A,B(C)} / L_{B,A(C)}$, which is a measure of the relative number of derived alleles found more often in population A compared to population B. We estimated the variance in $R_{A/B(C)}$ by running a Jackknife approach in blocks of 1000 from the set of sites in C. We compared the frequency of variants in historical and modern data as measured by $R_{A/B(C)}$ in two categories: 1) missense changes in the protein coding sequence, and 2) variants which are likely to cause loss of function.

To predict the likelihood of a variant being deleterious we used PolyPhen-2 (Figure 3C) [18]. This tool predicts the effects of amino acid substitutions on the structure and function of human proteins using a set of comparative and structural criteria. SNPs identified in the gorilla genome were lifted over to the human reference (hg38) using the command-line version of the liftOver tool (https://genome-store.ucsc.edu/) and the gorGor4ToHg38 chainfile available from UCSC (http://hgdownload.cse.ucsc.edu/goldenPath/gorGor4/liftOver/). Next, we used the PolyPhen-2 implementation of the Variant Effect Predictor tool to obtain PolyPhen-2 scores, with higher scores indicating a higher likelihood of an allele being damaging (scores above 0.45 indicate possibly damaging mutations). Finally, to obtain an estimate of the number of putatively damaging alleles in the historical and modern populations, we randomly subsampled an allele for each site among all individual from the respective population and retrieved the associated PolyPhen-2 score for each of these alleles.

For all identified LoF variants (see above) we obtained the historical and modern allele frequencies from the VCF-files and identified all LoF alleles with an absolute allele frequency difference between the modern and historical populations above 0.2 (see Data S2). For each of these LoF alleles we obtained the associated gene based on the human genome annotation by lifting over the variant to the human genome using the command-line version of the liftOver tool (https://genome-store.ucsc.edu/) and the gorGor4ToHg38 chainfile available from UCSC. We then assessed the functional enrichment of LoF variants with the highest difference in allele frequency between modern and historical populations in GOrilla [44] (see Data S3).

DATA AND SOFTWARE AVAILABILITY

The accession number for the FASTQ files reported in this paper is ENA: PRJEB29503.